Itinerant Magnetism in Metallic $CuFe_2Ge_2$

K. V. Shanavas*, David J. Singh

Oak Ridge National Laboratory, 1 Bethel Valley Road, Oak Ridge, Tennessee 37831, USA

* kavungalvees@ornl.gov

Abstract

Theoretical calculations are performed to understand the electronic structure and magnetic properties of $CuFe_2Ge_2$. The band structure reveals large electron density $N(E_F)$ at the Fermi level suggesting a strong itinerant character of magnetism. The Fermi surface is dominated by two dimensional sheet like structures, with potentially strong nesting between them. The magnetic ground state appears to be ferromagnetic along a and antiferromagnetic in other directions. These results show that $CuFe_2Ge_2$ is an antiferromagnetic metal, with similarities to the Fe-based superconductors; such as magnetism with substantial itinerant character and coupling between magnetic order and electrons at the Fermi energy.

Introduction

Discovery of superconductivity in copper oxides [1] and iron pnictides and chalcogenides [2] has generated interest in the coexistence and interplay of magnetism and superconductivity. [3] The Fe-based materials in particular show a close association of superconductivity and antiferromagnetism, with at least partial itinerant character and coupling of magnetism to electrons at the Fermi surface. [4]

Superconductivity in these systems is believed to be unconventional, in that it is mediated by antiferromagnetic spin-fluctuations. [5] The large spin-fluctuations may arise as a consequence of nearness to a quantum critical point (QCP), which can also lead to non-Fermi liquid behavior, unusual transport and novel ground states. [6] There is evidence for this both from comparison of standard density functional calculations with experiments and spectroscopic probes. [7, 8]

In any case, it is of interest to look for other materials that share similar characteristics. In this manuscript we present theoretical investigations of electronic and magnetic properties of $CuFe_2Ge_2$, to serve as a precursor to future experimental studies. Our study is motivated in part by recent experimental results for YFe_2Ge_2 which indicate superconductivity along with highly enhanced Fermi liquid properties and scalings characteristic of a material near a magnetic QCP. [9] We identified $CuFe_2Ge_2$ as a compound with similar structural characteristics and, as discussed below, find many other similarities at the standard density functional level. $CuFe_2Ge_2$ is readily prepared by arc melting and crystallizes in orthorhombic structure with two formula units per cell. [10] Although it differs from the layered $ThCr_2Si_2$ structure of the Fe-based superconductors with 122 stoichiometry, bond lengths and interactions exhibit several similarities. Our calculated electronic band structure in the non-spin-polarized phase shows

a large density of states at the Fermi level, consistent with itinerant character. Fermi surfaces in this system have a sheet like structure amenable to nesting and consequently to magnetic instabilities. Calculation of different magnetic configurations reveal significant variations in energies and $N(E_F)$ across them.

Methods

The calculations reported in this manuscript are performed within density functional theory (DFT) using plane wave basis set and pseudopotentials with the Vienna *ab-initio* simulation package. [11], [12] We use generalized gradient approximation (PBE-GGA) for exchange correlation. [13] The calculations are carried out with the energy cutoff of 400 eV and **k**-mesh of 16×20×12 after carefully checking for convergence. We also verified some of our calculations with the all electron code Wien2k, [14] to confirm that there are no artifacts of pseudopotential method.

The structure of CuFe$_2$Ge$_2$ was determined by Zavalii *et al* by x-ray powder diffraction on samples prepared through arc melting. [10] They found the material to crystallize in the orthorhombic structure, with space group $Pmma - D_{2h}^{16}$ and lattice constants (in Å) $a = 4.98$, $b = 3.97$ and $c = 6.77$. As shown in Fig. 1, the unitcell contains two formula units with Cu occupying the 2a sites. Fe occupies two inequivalent positions with the 2d ions (Fe$_1$) bonded octahedrally to surrounding Ge, while Fe at 2f sites (Fe$_2$) are bonded with four Cu ions on the ab plane and two Ge on the bc plane. Optimization of the experimental structure in the ferromagnetic phase yielded volume within 1% and atomic coordinates within 0.1 Å, which suggest that the theoretical equilibrium structure is very close to the experimental one. Note that nearest neighbor Fe-Fe distances are around 2.5 Å (Fig. 2), which is shorter than the 2.8 Å in YFe$_2$Ge$_2$, and suggests that direct Fe-Fe interactions will be important in this system as well.

Results

Electronic structure

As can be seen from the non-spin-polarized GGA bandstructure in Fig. 3, the states close to Fermi level are dominated by Fe-3d levels. Absence of strong crystal field splitting in the Fe-d states point to the fact that the direct Fe-Fe interactions dominate, a character common to other iron-based superconductors. [15], [16] From the band character plot we can see that Fe$_1$ and Fe$_2$ exhibit different dispersions close to Fermi level. For the directions plotted, the Fe$_1$ bands remain relatively flat and this leads to a higher density of octahedral Fe$_1$-3d levels near Fermi energy as can be seen from the partial density of states plotted in Fig. 4. The Fe$_2$ bands show relative large dispersions along $\Gamma-Y$ and $\Gamma-Z$ directions, suggesting a three dimensional nature of the band structure. The Cu-3d levels lie between -5 and -2 eV relative to Fermi level and thus are fully occupied, which can also be seen from Fig. 4. Nearly all Fe and Cu 4s characters lie above the Fermi level. Counting the occupied states with different characters suggests nominal occupations of Cu 3d^{10}, Fe 3$d^{7.5}$ and Ge 4$s^2$4p^3.

The densities of states (Fig. 4) also show features similar to YFe$_2$Ge$_2$ and the Fe-based superconductors [15], [17] such as the dip in the DOS just above E_F. The calculated electronic DOS at the Fermi level, $N(E_F)$, is also high at $N(E_F) = 7.9$ eV^{-1} per formula unit. This corresponds to a bare Sommerfeld specific heat coefficient $\gamma_{\text{bare}} = 18.6$ mJ/(mol K^2), which is in fact higher than the calculated value for YFe$_2$Ge$_2$. The contribution from different Fe sites to $N(E_F)$ are found to be significantly different; we get 5.2 eV^{-1} and 1.6 eV^{-1} respectively for Fe$_1$ and Fe$_2$. This suggest that the octahedrally coordinated Fe$_1$ has a higher tendency for itinerant magnetism in this
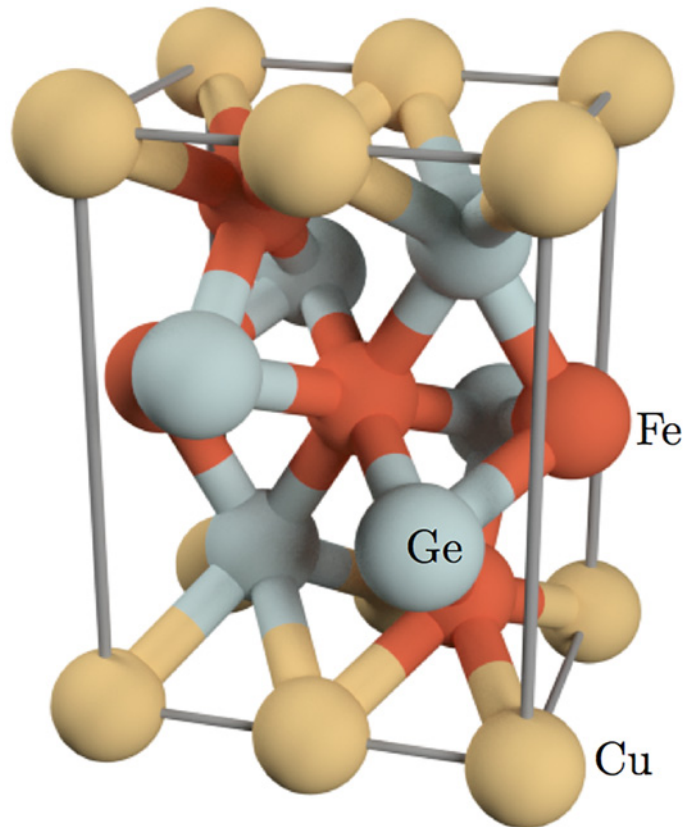
Fig 1. The crystal structure of CuFe$_2$Ge$_2$. It shows the orthorhombic unitcell containing two formula units.
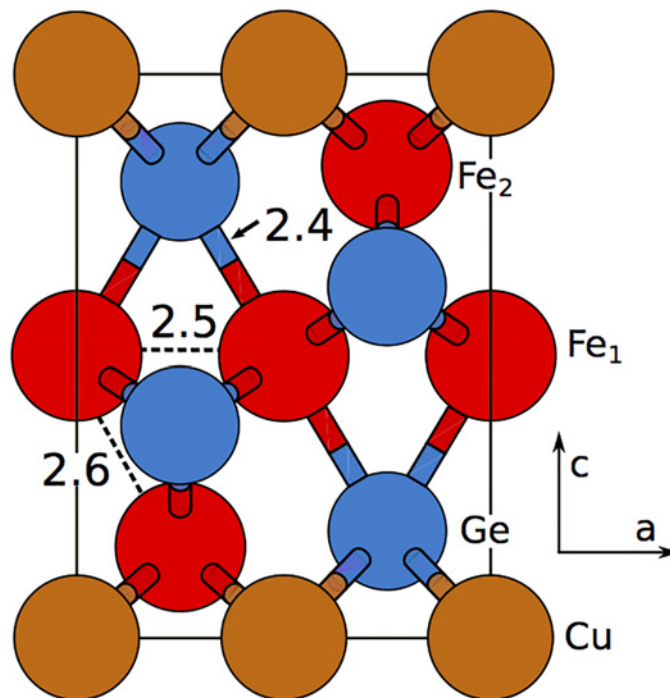
Fig 2. The projection of CuFe$_2$Ge$_2$ unitcell on to *ac* plane. Fe$_1$ (middle layer) are octahedrally coordinated. The atomic distances are marked in Angstrom.
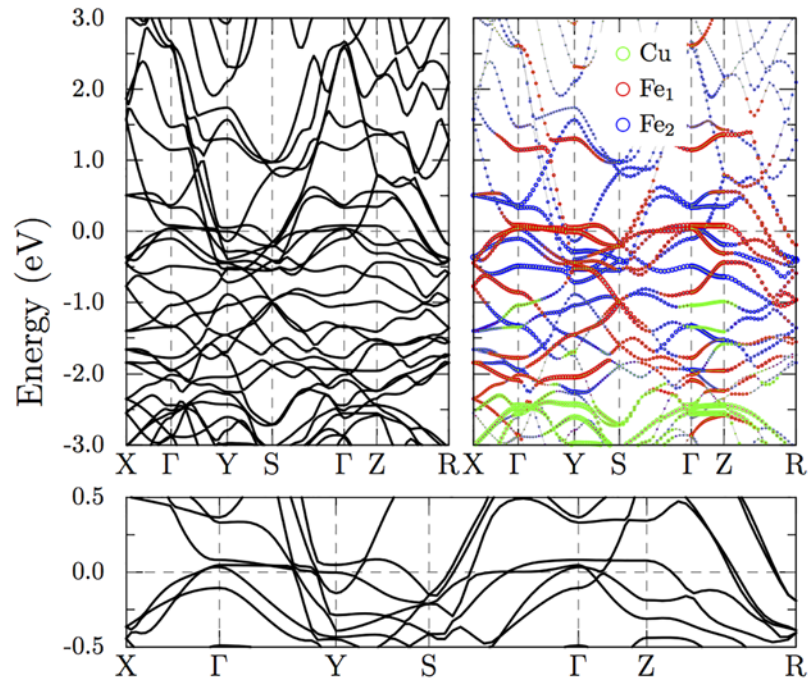
Fig 3. Electronic band structure of CuFe$_2$Ge$_2$ in the non-magnetic phase calculated using GGA. The bottom panel zooms in on the states close to Fermi level which is set to 0 eV. The orbital character of the bands are shown by colored symbols in the top right panel. States close to Fermi level are dominated by Fe-3d states.

doi:10.1371/journal.pone.0121186.g003

material. The contributions from different d orbitals of Fe ions are shown in Fig. 5. As we can see, various states contribute towards density near the Fermi level similar to Fe pnictides.

The calculated Fermi surfaces in the paramagnetic phase is shown in Fig. 6. There are seven bands that cross Fermi level and all of them have strong Fe-d character as can be seen from Fig. 3. The Fermi surfaces are dominated by four mostly flat sheets in the a^* b^* plane of the reciprocal space. Out of these the first three (3, 4, 5) have strong Fe$_1$ character. The closest of these, the pair marked by "3" in Fig. 6 are separated by half the reciprocal space distance b^*. We can expect strong nesting between these bands which may lead to antiferromagnetic coupling between Fe moments along the b axis. In addition to the sheets perpendicular to the b^* axis, there are also a hole pocket (1) at the Γ point and an elongated disk shaped electron pocket (7) around S and a dumbbell shaped structure (2) along a^*.

Magnetism

The large density of states at the Fermi level $N(E_F)$, discussed earlier, implies that this system has magnetic instabilities as per the Stoner criterion. Certain itinerant systems, such as YFe$_2$Ge$_2$, do not order magnetically even though DFT calculations predict magnetic ground state. [15, 17] Large spin-fluctuations are believed to be responsible for this effect, which happens in systems close to a QCP, and this leads to interesting new physics in these systems. [9] DFT is known to overestimate magnetic tendencies in itinerant systems close to QCPs because the exchange-correlation functionals commonly employed are based on the properties of the uniform electron gas which neglects the spin fluctuations associated with the QCP. [6] However, we are not aware of any magnetic measurements of CuFe$_2$Ge$_2$.
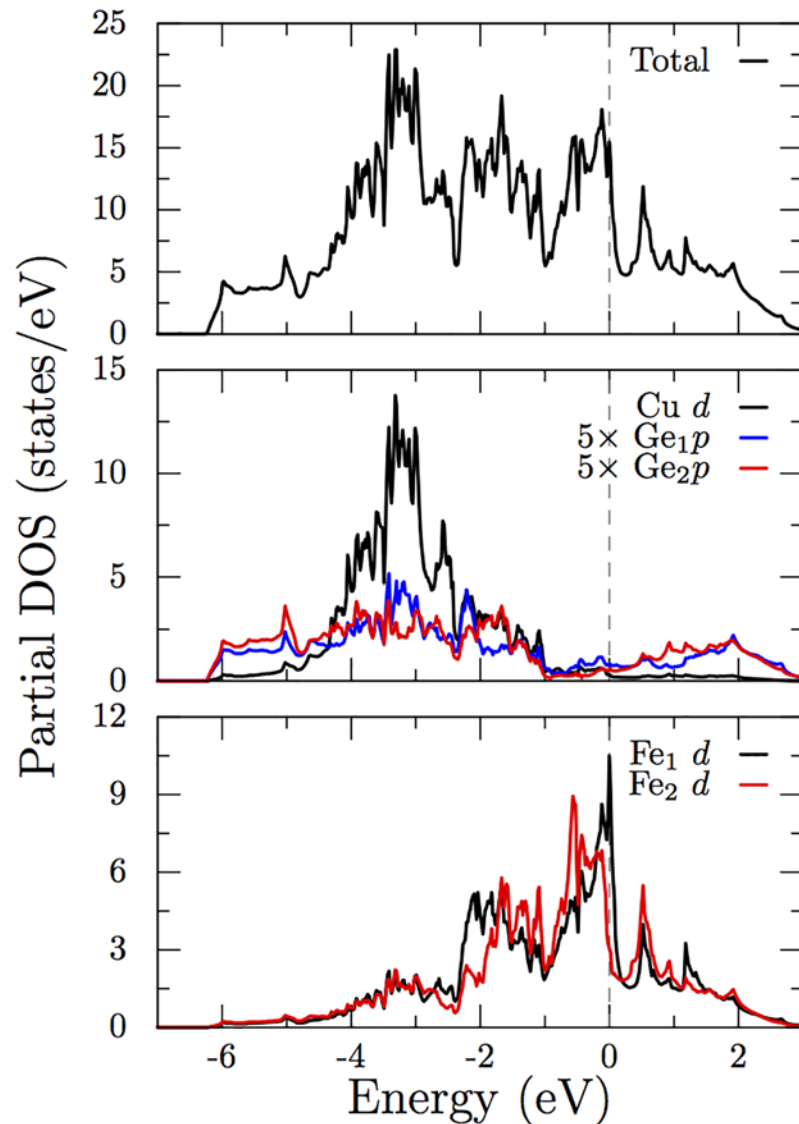
Fig 4. Total and partial density of states (DOS) for the non-magnetic calculation. Cu-*d* states are below the fermi level while Fe-*d* and Ge-*p* are partially occupied. Not shown are Fe and Cu *s* states, that are empty.

Thus, we carried out spin polarized calculations in several magnetic configurations and find that a ferromagnetic state is lower in energy by 102 meV/f.u. compared to non-spin-polarized state. A magnetic moment of about 1.4 μ_B develops on the Fe atoms and the $N(E_F)$ drops to about 4.1 eV^{-1}. For comparison, we also calculated other magnetic structures and the results are listed in Table 1, and explained as follows. In the AF-*c*1, the Fe planes are arranged antifer-romagnetically along the *c* direction and ferromagnetic in other directions. In AF-*c*2 the Fe$_1$-Fe$_2$ coupling is AFM along *c*, but Fe$_1$-Fe$_1$ is FM. The AF-*b* is AFM along the *b* direction and we find that a similar AF-*a* could not be stabilized. The AF-*C* corresponds to checkerboard ar-rangement of moments in the *ab* plane. Finally, AF-*G* is obtained by starting from a different configuration and turns out to have the lowest energy. It is similar to AF-*c*2, except that it is also AFM along the *b* direction.
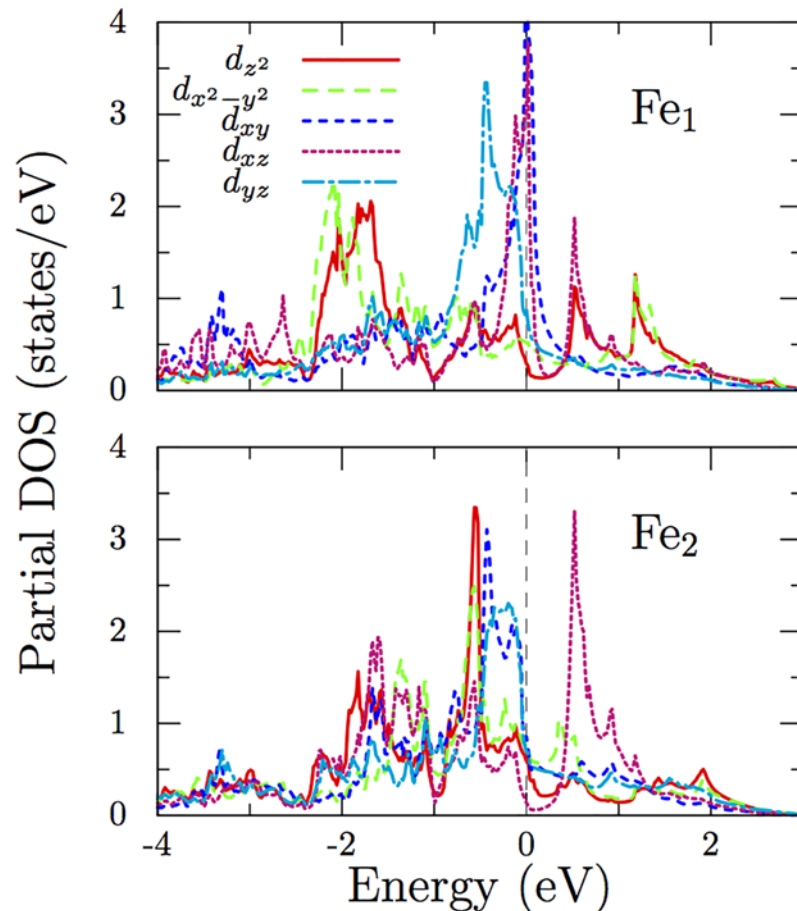
Fig 5. Partial density of states for Fe-*d* states. Contributions from the *d* states of Fe$_1$ and Fe$_2$ ions near the Fermi level from the non-magnetic calculation show that all states contribute significantly to the density of states. The crystallographic axes are taken as the coordinate system for calculation.

The large variations in energies and $N(E_F)$ across the ordered magnetic configurations suggest itinerant character of Fe moments. Note in particular that the difference in energy between different magnetic orders is as much as 0.11 eV/f.u., which is more than half the as much energy difference between a non-spin-polarized calculation and the lowest energy state and that the values of $N(E_F)$ also vary over a large range depending on the particular order. Moreover, the lowest energy configuration AF-*G* is only 18 meV lower than the next lowest configuration. In our calculations, FM and AF-*b* structures have similar energies, which suggest that magnetic exchange along *b* direction is small. However, AF-*G* is lower than AF-*c*2 by about 50 meV/f.u., while the difference between the two cases is AFM along *b*. This also suggests that a Heisenberg type model with nearest neighbor interactions will not fit this system.

Finally, we also calculated magnetic phases with local density approximation (LDA). It has been found that for itinerant systems near QCP, calculations with LDA predict much weaker magnetic tendencies. [7, 17] This corresponds to a relative weakness of the momentum formation. Indeed, we find that the Fe moments in the FM configuration are 0.98 and 0.48 μ_B within LDA which are much smaller than the GGA moments of 1.44 and 1.40 μ_B respectively, as given in Table 1.
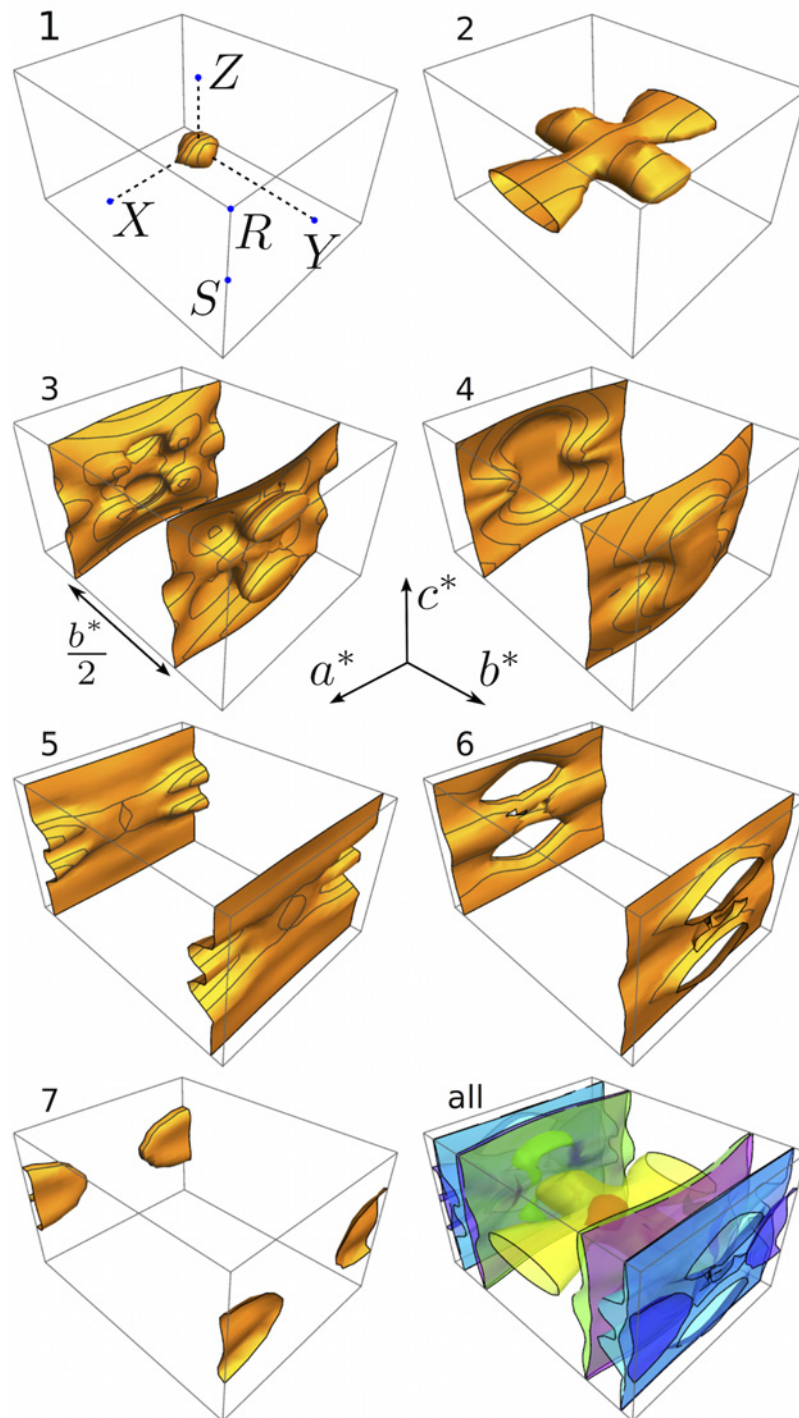
Fig 6. Calculated Fermi surfaces of CuFe$_2$Ge$_2$. The high symmetry points are marked in the first panel. Seven bands with Fe-*d* character cross Fermi level and bands numbered as 1, 3, 4, 5 have strong Fe$_1$ character and bands 2, 6, 7 have strong Fe$_2$ character.

Table 1. Magnetic properties from GGA.

Order	m_{Fe1} (μ_B)	m_{Fe2} (μ_B)	E (eV/f.u.)	$N(E_F)$
NSP	0.00	0.00	0.00	7.91
FM	1.44	1.40	-0.10	4.13
AF-c1	1.28	1.22	-0.15	3.36
AF-c2	1.32	1.30	-0.16	3.49
AF-b	1.52	1.40	-0.10	4.72
AF-C	1.45	1.41	-0.19	2.86
AF-G	1.40	1.45	-0.21	3.04

For different magnetic ordering patterns studied (see text), the resulting magnetic moments m, energies and density at the Fermi surface $N(E_F)$ in units of eV^{-1} per formula unit. The energy of paramagnetic case (NSP) is taken to be zero.

doi:10.1371/journal.pone.0121186.t001

Discussion

Our theoretical calculations on CuFe$_2$Ge$_2$ suggest that this material is an interesting itinerant magnetic system. The electronic structure shows similarities with those of the Fe-based superconductors. The Fermi surfaces show parallel sheet-like structures with potential nesting induced instabilities. Several magnetic configurations are stable, but the lowest energy is reached when Fe moments are ferromagnetic along a and antiferromagnetic along b and c directions. On the scale of moment formation energy, there are significant variations in energies and densities of states at the Fermi level between different magnetic configurations, which also points to itinerant character in this system. We believe CuFe$_2$Ge$_2$ deserves further experimental investigation.

Acknowledgments

Author Contributions

Conceived and designed the experiments: KVS DJS. Performed the experiments: KVS DJS. Analyzed the data: KVS DJS. Wrote the paper: KVS DJS.

References

1. Fujita M, Hiraka H, Matsuda M, Matsuura M, M Tranquada J, Wakimoto S, et al. Progress in Neutron Scattering Studies of Spin Excitations in High-T_c Cuprates. J Phys Soc Jpn. 2012 Jan; 81(1):011007. Available from: http://dx.doi.org/10.1143/JPSJ.81.011007.

2. Stewart GR. Superconductivity in iron compounds. Rev Mod Phys. 2011 Dec; 83(4):1589. Available from: http://dx.doi.org/10.1103/RevModPhys.83.1589.

3. Dai P, Hu J, Dagotto E. Magnetism and its microscopic origin in iron-based high-temperature superconductors. Nat Phys. 2012 Oct; 8(10):709. Available from: http://dx.doi.org/10.1038/nphys2438.

4. Chen GF, Li Z, Wu D, Li G, Hu WZ, Dong J, et al. Superconductivity at 41 K and Its Competition with Spin-Density-Wave Instability in Layered CeO$_{1-x}$F$_x$FeAs. Phys Rev Lett. 2008 Jun; 100:247002. Available from: http://link.aps.org/doi/10.1103/PhysRevLett.100.247002. PMID: 18643616

5. Mazin II, Singh DJ, Johannes MD, Du MH. Unconventional Superconductivity with a Sign Reversal in the Order Parameter of LaFeAsO$_{1-x}$F$_x$. Phys Rev Lett. 2008 Jul; 101(5):057003. Available from: http://dx.doi.org/10.1103/PhysRevLett.101.057003. PMID: 18764420

6. Aguayo A, Mazin II, Singh DJ. Why Ni_3Al Is an Itinerant Ferromagnet but Ni_3Ga Is Not. Phys Rev Lett. 2004 Apr; 92(14):147201. Available from: http://dx.doi.org/10.1103/PhysRevLett.92.147201. PMID: 15089568

7. Mazin II, Johannes MD, Boeri L, Koepernik K, Singh DJ. Problems with reconciling density functional theory calculations with experiment in ferropnictides. Phys Rev B. 2008 Aug; 78:085104. Available from: http://link.aps.org/doi/10.1103/PhysRevB.78.085104.

8. Bondino F, Magnano E, Malvestuto M, Parmigiani F, McGuire MA, Sefat AS, et al. Evidence for Strong Itinerant Spin Fluctuations in the Normal State of $CeFeAsO_{0.89}F_{0.11}$ Iron-Oxypnictide Superconductors. Phys Rev Lett. 2008 Dec; 101:267001. Available from: http://link.aps.org/doi/10.1103/PhysRevLett.101.267001. PMID: 19113783

9. Zou Y, Feng Z, Logg PW, Chen J, Lampronti G, Grosche FM. Fermi liquid breakdown and evidence for superconductivity in YFe_2Ge_2. Phys Status Solidi RRL. 2014 Sep; 9999 (9999):1. Available from: http://dx.doi.org/10.1002/pssr.201409418.

10. Zavalii IY, Pecharskii VK, Bodak OI. Crystal structure of the compounds $CuFe_2Ge_2$ and $Cu_{1\pm x}Co_{2\mp x}Ge_2$. Kristallografiâ. 1987; 32:66. Rus. Available from: http://www.refdoc.fr/Detailnotice?idarticle=13508415.

11. Kresse G, Hafner J. Ab-initio molecular dynamics for liquid metals. Phys Rev B. 1993 Jan; 47(1):558. Available from: http://dx.doi.org/10.1103/PhysRevB.47.558.

12. Kresse G. Efficient iterative schemes for ab initio total-energy calculations using a plane-wave basis set. Phys Rev B. 1996 Oct; 54(16):11169. Available from: http://dx.doi.org/10.1103/PhysRevB.54.11169.

13. Perdew JP, Burke K, Wang Y. Generalized gradient approximation for the exchange-correlation hole of a many-electron system. Phys Rev B. 1996 Dec; 54:16533. Available from: http://link.aps.org/doi/10.1103/PhysRevB.54.16533.

14. Blaha P, Schwarz K, Madsen GKH, Kvasnicka D, Luitz J. WIEN2k, An Augmented PlaneWave + Local Orbitals Program for Calculating Crystal Properties. Karlheinz Schwarz, Techn. Universit at Wien, Austria; 2001.

15. Subedi A. Unconventional sign-changing superconductivity near quantum criticality in YFe_2Ge_2. Phys Rev B. 2014 Jan; 89(2):024504. Available from: http://dx.doi.org/10.1103/PhysRevB.89.024504.

16. Singh DJ, Du MH. Density Functional Study of $LaFeAsO_{1-x}F_x$: A Low Carrier Density Superconductor Near Itinerant Magnetism. Phys Rev Lett. 2008 Jun; 100(23):237003. Available from: http://dx.doi.org/10.1103/PhysRevLett.100.237003. PMID: 18643537

17. Singh DJ. Superconductivity and magnetism in YFe_2Ge_2. Phys Rev B. 2014 Jan; 89(2):024505. Available from: http://dx.doi.org/10.1103/physrevb.89.024505.